Bounded UDE-Based Control for a SLAM Equipped Quadrotor with Input Constraints

Yafeng Wang, Yeqin Wang, Yiting Dong and Beibei Ren

***Abstract*—Simultaneous Localization and Mapping (SLAM) system equipped quadrotors are preferable candidates for autonomous building inspections and surveillance tasks, because of their mobility and capability of working in both indoor and outdoor environments. However, the lack of robustness still remains as one of the challenging problems of SLAM implementations. Sudden camera moving, motion blur, occlusion all might cause a pose lost and map corruption. This problem becomes significant when the SLAM system is mounted on a quadrotor, since the high agility of the quadrotor might lead to a wide camera motion. Therefore, a control strategy that can constrain the quadrotor motion angles is proposed in this paper. A bounded design is embedded into the existing uncertainty and disturbance estimator (UDE) control framework, which can regulate the motion angles, e.g., roll and pitch angles of the quadrotor, always within predefined appropriate ranges. The proposed control strategy eliminates the sudden camera motion and provides a suitable platform for SLAM. Finally, experimental studies are provided for validation.**

I. Introduction

Impressive achievement in camera based-Simultaneous Localization and Mapping (SLAM) has been made in past decades [1], [2], [3]. As a novel localization approach, SLAM releases numerous limitations of the Global Positioning System (GPS), i.e., drifting and GPS dependency [4]. However, the lack of robustness still remains as one of the challenging problems of SLAM implementations. Sudden camera moving, motion blur, occlusion all might cause a pose lost and map corruption [5]. A general approach to solve the pose lost problem of SLAM is the re-localization technique [6], [7], [8], [9], which guarantees the SLAM to automatically detect and recover from tracking failures. Although the re-localization technique can handle most of the experimental scenarios, it might not work effectively for a quadrotor carried SLAM, because an instant position lost aerially may lead to failures in flight control.

This paper proposes a novel strategy to eliminate the sudden motion of a quadrotor, and further provides a suitable platform for SLAM. In particular, the pose lost problem of the quadrotor carried SLAM is reformulated as a quadrotor control problem with input constraints. The constraint control problem of quadrotors has been extensively explored in literature. The general way to regulate the control signal is by adding a saturation unit [10]. This method is straightforward and easy to be implemented, however, might lead to the instability problem. Meanwhile, there are many other technical approaches to solve the quadrotor control problem with input constraints. In [11], a control Lyapunov function (CLF) is introduced for the output constrained case, such that the velocity and the heading rate can be constrained within specific ranges. In [12], an inner-outer loop control framework is developed, where the outer loop (position control) generates a saturated reference signal for the inner loop (attitude control), and the inner loop is designed to track the reference signal using a traditional proportional-integral-derivative (PID) controller. Besides, the full state constraint is successfully handled using the bang-bang control [13] and the barrier Lyapunov function method [14]. In [15], the quadrotor nonlinearity problem is investigated with reinforcement learning, and the controller output saturation is addressed by introducing $\tanh(\cdot)$ functions. Although previous research works have handled the quadrotor control with input constraints, a control system specifically designed for the SLAM system is not explored.

Other challenges for the quadrotor control come from its highly nonlinear dynamics, parametric uncertainties, and external disturbances. In recent years, a robust control method, uncertainty and disturbance estimator (UDE)-based control [16], has been successfully applied to the quadrotor control to handle uncertainties, nonlinear effects, disturbances [17], [18], [19]. Though the robust performance of quadrotor control is achieved, the input constraints are not considered in these designs.

This paper proposes a novel strategy to eliminate the sudden motion for a SLAM equipped quadrotor, and further provides a suitable platform for SLAM. In particular, the pose lost problem of a quadrotor carried SLAM is reformulated as a quadrotor control problem with input constraints. Inspired by [20], a bounded UDE-based controller is proposed for the SLAM system equipped quadrotor. The main contributions of this paper are summarized as follows:

- A bounded design is embedded into the UDE control framework to form a bounded UDE-based position controller for a quadrotor with input constraints to deal with the pose lost problem of SLAM. With the implementation of the proposed control strategy, both roll and pitch angles of the quadrotor are regulated within predefined appropriate ranges, and further providing a suitable platform for SLAM.
- The UDE-based control method is applied for the

Yafeng Wang, Yiting Dong, and Beibei Ren are with the Department of Mechanical Engineering, Texas Tech University, Lubbock, TX 79409, USA. e-mail: yafeng.wang@ttu.edu, yiting.dong@ttu.edu, beibei.ren@ttu.edu.

Yeqin Wang is with the National Wind Institute, Texas Tech University, Lubbock, TX 79409, USA. e-mail: yeqin.wang@ttu.edu.

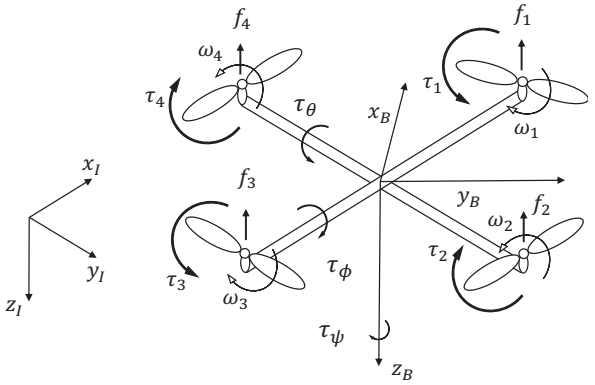

Figure 1. Coordinate systems for a quadrotor model

quadrotor to handle the coupling effects, model uncertainties, and external disturbances.

The rest of this paper is organized as follows. In Section II, the dynamic model of a quadrotor and the control objective are provided. The UDE-based attitude controller and the bounded UDE-based position controller are developed in Section III. The experimental validation is given in Section IV followed by conclusion remarks in Section V.

II. Dynamic Modeling and Problem Formulation

A. Dynamic Modeling of a Quadrotor

In this paper, a quadrotor is investigated as shown in Fig. 1, which consists of four rotors as action actuators. Both positions and attitudes can be controlled by tuning the rotation speeds of those rotors. The model used in this paper satisfies the following assumptions: the quadrotor body frame is rigid, and the gravity center and the geometric center are coincident. The thrust f_k and the torque τ_k on each rotor are given as $f_k = h_F w_k^2$ and $\tau_k = h_M w_k^2$, where $k = 1, \cdots, 4$, represents the rotor index, w_k is the angular velocity of each rotor, h_F and h_M are positive drag constants. Let l denote the arm length of the quadrotor.The torques τ_ϕ, τ_θ, τ_ψ along x_B, y_B and z_B axes, respectively, and the total lift force F can be represented as

$$\tau_\phi = l\left(f_4 - f_2\right) = h_F l\left(w_4^2 - w_2^2\right) \quad (1)$$

$$\tau_\theta = l\left(f_1 - f_3\right) = h_F l\left(w_1^2 - w_3^2\right) \quad (2)$$

$$\tau_\psi = \tau_2 + \tau_4 - \tau_1 - \tau_3 = h_M\left(w_2^2 + w_4^2 - w_1^2 - w_3^2\right) \quad (3)$$

$$F = f_1 + f_2 + f_3 + f_4 = h_F\left(w_1^2 + w_2^2 + w_3^2 + w_4^2\right) \quad (4)$$

Considering the bounded disturbance signals $d_{\eta i}$, $i = 1, 2, 3$, on roll, pitch, yaw angles, respectively, and $d_{\xi j}$, $j = 1, 2, 3$, on x_B, y_B and z_B axes, respectively, the dynamic model of a quadrotor can be represented as [18]

$$\ddot{\phi} = \left[\frac{\tau_\phi}{I_x} + \left(\frac{I_y - I_z}{I_x}\right)\dot{\theta}\dot{\psi} - \frac{J\dot{\theta}\Omega}{I_x}\right] + d_{\eta 1} \quad (5)$$

$$\ddot{\theta} = \left[\frac{\tau_\theta}{I_y} + \left(\frac{I_z - I_x}{I_y}\right)\dot{\phi}\dot{\psi} - \frac{J\dot{\phi}\Omega}{I_y}\right] + d_{\eta 2} \quad (6)$$

$$\ddot{\psi} = \left[\frac{\tau_\psi}{I_z} + \left(\frac{I_x - I_y}{I_z}\right)\dot{\theta}\dot{\phi}\right] + d_{\eta 3} \quad (7)$$

$$\ddot{x} = -\frac{F}{m}\left[\cos\psi\sin\theta\cos\phi + \sin\psi\sin\phi\right] + d_{\xi 1} \quad (8)$$

$$\ddot{y} = -\frac{F}{m}\left[\sin\psi\sin\theta\cos\phi - \cos\psi\sin\phi\right] + d_{\xi 2} \quad (9)$$

$$\ddot{z} = -\frac{F}{m}\left[\cos\theta\cos\phi\right] + g + d_{\xi 3} \quad (10)$$

where (5)-(7) is the attitude subsystem, (8)-(10) is the position subsystem, g is the gravitational acceleration, m is the mass, J denotes the inertia of propellers, ϕ, θ, ψ are the roll, pitch and yaw angles, respectively, I_x, I_y, I_z are the moments of inertia along the x_B, y_B and z_B axes, and $\Omega = w_2 + w_4 - w_1 - w_3$.

To simplify the control design, define $\eta_1 = \phi$, $\eta_2 = \theta$, $\eta_3 = \psi$. The dynamics of the attitude subsystem (5)-(7) can be rewritten as

$$\ddot{\eta}_i = D_{\eta i} + B_{\eta i} u_{\eta i} \quad (i = 1,\ 2,\ 3) \quad (11)$$

where $B_{\eta 1} = \frac{1}{I_x}$, $B_{\eta 2} = \frac{1}{I_y}$, $B_{\eta 3} = \frac{1}{I_z}$, $u_{\eta 1} = \tau_\phi$, $u_{\eta 2} = \tau_\theta$, $u_{\eta 3} = \tau_\psi$, $D_{\eta i}$ denote the lumped uncertainty terms

$$D_{\eta 1} = \frac{1}{I_x}\left[\left(I_y - I_z\right)\dot{\theta}\dot{\psi} - J\dot{\theta}\Omega\right] + d_{\eta 1} \quad (12)$$

$$D_{\eta 2} = \frac{1}{I_y}\left[\left(I_z - I_x\right)\dot{\phi}\dot{\psi} - J\dot{\phi}\Omega\right] + d_{\eta 2} \quad (13)$$

$$D_{\eta 3} = \frac{1}{I_z}\left[\left(I_x - I_y\right)\dot{\theta}\dot{\phi}\right] + d_{\eta 3} \quad (14)$$

with $\left(I_y - I_z\right)\dot{\theta}\dot{\psi}$, $\left(I_z - I_x\right)\dot{\phi}\dot{\psi}$, $\left(I_x - I_y\right)\dot{\theta}\dot{\phi}$ being the coupling terms.

By choosing the coordinates as $\xi_1 = x$, $\xi_2 = y$, $\xi_3 = z$, the dynamics of the position subsystem (8)-(10) can be rewritten as

$$\ddot{\xi}_j = -B_{\xi j} u_{\xi j} + D_{\xi j} + \hat{g}_j \quad (j = 1,\ 2,\ 3) \quad (15)$$

where $\hat{g}_1 = \hat{g}_2 = 0$, $\hat{g}_3 = g$ is the gravitational acceleration, $B_{\xi 1} = B_{\xi 2} = F/m$, $B_{\xi 3} = 1/m$, $u_{\xi 1} = u_x$, $u_{\xi 2} = u_y$, $u_{\xi 3} = F$ are the position control inputs, and $D_{\xi j}$ denote the lumped uncertainty terms

$$D_{\xi 1} = -\frac{F}{m}\left[\cos\psi\sin\theta\cos\phi + \sin\psi\sin\phi - u_x\right] + d_{\xi 1} \quad (16)$$

$$D_{\xi 2} = -\frac{F}{m}\left[\sin\psi\sin\theta\cos\phi - \cos\psi\sin\phi - u_y\right] + d_{\xi 2} \quad (17)$$

$$D_{\xi 3} = \frac{F}{m}\left[1 - \cos\theta\cos\phi\right] + d_{\xi 3} \quad (18)$$

B. Control Objective

The control objective of this work is to develop a robust control strategy to regulate the position of a SLAM equipped quadrotor $[x,\ y,\ z]$ to their reference signals $[x_r,\ y_r,\ z_r]$. Meanwhile, the system states, roll and pitch angles, will be constrained as $\phi \in (-\phi_{max},\ \phi_{max})$, $\theta \in (-\theta_{max},\ \theta_{max})$, where $\phi_{max} > 0$ and $\theta_{max} > 0$ are the constraint values, which can be determined by experimental testings to avoid the SLAM pose lost. The large rotation on roll and pitch angles is the main reason of the SLAM pose lost.

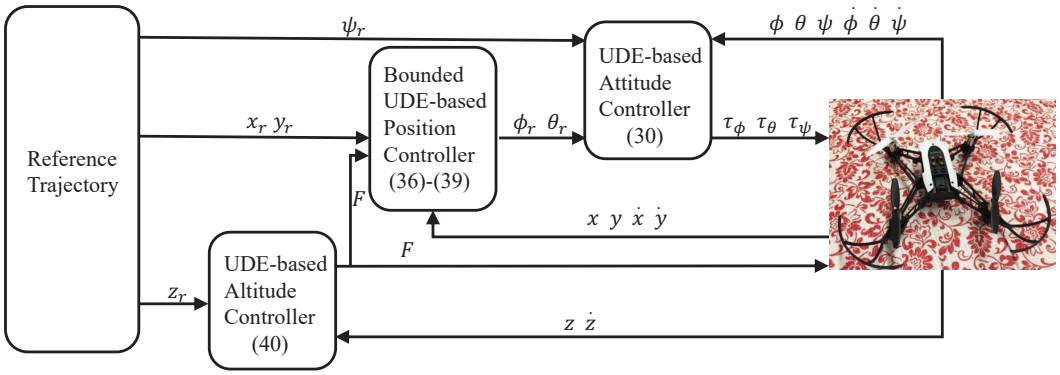

Figure 2. The cascaded inner-outer loop control scheme

III. Control Design

In this section, a cascaded inner-outer loop control scheme, as shown in Fig. 2, is developed for a SLAM equipped quadrotor. The inner UDE-based attitude controller is to control the states $[\phi,\, \theta,\, \psi]$ to track the reference signals $[\phi_r,\, \theta_r,\, \psi_r]$. The outer position controller consists of a bounded UDE-based position controller and a UDE-based altitude controller. The bounded UDE-based position controller is to drive the states $[x,\, y]$ to track the reference signals $[x_r,\, y_r]$ and generate the reference signals ϕ_r and θ_r for the attitude controller. The altitude controller is to drive the state z to track the reference signal z_r.

A. Inner Attitude Control

Define $\eta_{r1} = \phi_r$, $\eta_{r2} = \theta_r$, $\eta_{r3} = \psi_r$. The tracking errors of the attitude subsystem (5)-(7) and their derivatives can be represented as

$$e_{\eta i} = \eta_{ri} - \eta_i \tag{19}$$

$$\dot{e}_{\eta i} = \dot{\eta}_{ri} - \dot{\eta}_i \quad (i = 1,\, 2,\, 3) \tag{20}$$

Define the filtered tracking error as

$$\varepsilon_{\eta i} = \lambda_{\eta i} e_{\eta i} + \dot{e}_{\eta i} \tag{21}$$

where $\lambda_{\eta i}$ are positive constants. Taking the time derivative of (21) along with (11) yields

$$\dot{\varepsilon}_{\eta i} = \lambda_{\eta i}\dot{e}_{\eta i} + \ddot{\eta}_{ri} - D_{\eta i} - B_{\eta i} u_{\eta i} \tag{22}$$

Consider the desired error dynamics as

$$\dot{\varepsilon}_{\eta i} = -k_{\eta i}\varepsilon_{\eta i} \tag{23}$$

where $k_{\eta i}$ are positive constants. Substituting (23) into (22), $u_{\eta i}$ can be designed as

$$u_{\eta i} = B_{\eta i}^{-1}\left[\lambda_{\eta i}\dot{e}_{\eta i} + \ddot{\eta}_{ri} - D_{\eta i} + k_{\eta i}\varepsilon_{\eta i}\right] \tag{24}$$

Define

$$u_{\eta i}^d = -D_{\eta i} \tag{25}$$

The desired error dynamics (23) can be rewritten as

$$\dot{\varepsilon}_{\eta i} = -k_{\eta i}\varepsilon_{\eta i} - D_{\eta i} - u_{\eta i}^d \tag{26}$$

Then

$$D_{\eta i} = -\dot{\varepsilon}_{\eta i} - k_{\eta i}\varepsilon_{\eta i} - u_{\eta i}^d \tag{27}$$

which indicates that the uncertainty term $D_{\eta i}$ could be estimated by the filtered tracking error $\varepsilon_{\eta i}$. By using the UDE technique in [18] and introducing a strictly proper filter $G_{\eta i}^f(s)$, the uncertainty terms $D_{\eta i}$ could be approximated as

$$\hat{D}_{\eta i} = \mathcal{L}^{-1}\left[G_{\eta i}^f(s)\right] * \left[-\dot{\varepsilon}_{\eta i} - k_{\eta i}\varepsilon_{\eta i} - u_{\eta i}^d\right] \tag{28}$$

where $\mathcal{L}^{-1}(\cdot)$ is the inverse-Laplace transform operator and $*$ is the convolution operator. Then substituting $u_{\eta i}^d = -\hat{D}_{\eta i}$ into (28) and solving $u_{\eta i}^d$ generates

$$u_{\eta i}^d = \mathcal{L}^{-1}\left[\frac{G_{\eta i}^f(s)}{1 - G_{\eta i}^f(s)}\right] * \left[\dot{\varepsilon}_{\eta i} + k_{\eta i}\varepsilon_{\eta i}\right]. \tag{29}$$

Combining (24) and (29) leads to the UDE-based attitude controller as

$$u_{\eta i} = B_{\eta i}^{-1}\Big\{k_{\eta i}\varepsilon_{\eta i} + \lambda_{\eta i}\dot{e}_{\eta i} + \ddot{\eta}_{ri} + \mathcal{L}^{-1}\left[\frac{G_{\eta i}^f(s)}{1 - G_{\eta i}^f(s)}\right] * \left[\dot{\varepsilon}_{\eta i} + k_{\eta i}\varepsilon_{\eta i}\right]\Big\} \tag{30}$$

B. Outer Position Control with Bounded Design

Considering the desired trajectories given as $\xi_{r1} = x_r$, $\xi_{r2} = y_r$, $\xi_{r3} = z_r$, the tracking errors of the position subsystem (8)-(10), and their derivatives are specified as

$$e_{\xi j} = \xi_{rj} - \xi_j \tag{31}$$

$$\dot{e}_{\xi j} = \dot{\xi}_{rj} - \dot{\xi}_j \quad (j = 1,\, 2,\, 3) \tag{32}$$

Define the filtered tracking error as

$$\varepsilon_{\xi j} = \lambda_{\xi j} e_{\xi j} + \dot{e}_{\xi j} \tag{33}$$

where $\lambda_{\xi j}$ are positive constants. Consider the desired error dynamics as

$$\dot{\varepsilon}_{\xi j} = -k_{b\xi j} k_{\xi j}\varepsilon_{\xi j} \tag{34}$$

where $k_{b\xi 1}$ and $k_{b\xi 2}$ are positive time-varying parameters which will be designed later, and $k_{b\xi 3} = 1$. Following the similar design process of the attitude controller, the UDE-

based position controller can be obtained as

$$u_{\xi j} = B_{\xi j}^{-1}\hat{g}_j - B_{\xi j}^{-1}\Big\{k_{b\xi j}k_{\xi j}\varepsilon_{\xi j} + \lambda_{\xi j}\dot{e}_{\xi j} + \ddot{\xi}_{rj} + \mathcal{L}^{-1}\left[\frac{G_{\xi j}^{f}(s)}{1-G_{\xi j}^{f}(s)}\right] * \left[\dot{\varepsilon}_{\xi j} + k_{b\xi j}k_{\xi j}\varepsilon_{\xi j}\right]\Big\} \quad (35)$$

where $\hat{g}_1 = \hat{g}_2 = 0$, $\hat{g}_3 = g$ is the gravitational acceleration. According to [20], the bounded design is embedded into (35) for $j = 1,\ 2$, and thus the bounded UDE-based position control θ_r and ϕ_r are proposed as

$$\theta_r = \frac{u_{b1}}{K_x} \quad (36)$$

$$\phi_r = -\frac{u_{b2}}{K_y} \quad (37)$$

where $K_x > 0$ and $K_y > 0$ are control gains, and the virtual outputs u_{bj} are designed as

$$\dot{u}_{bj} = -c_{1\xi j}u_{bj}\left(\frac{u_{bj}^2}{u_{\xi jmax}^2} + k_{b\xi j}^2 - 1\right) - c_{2\xi j}k_{b\xi j}^2\left(u_{bj} - u_{\xi j}\right) \quad (38)$$

$$\dot{k}_{b\xi j} = -c_{1\xi j}k_{b\xi j}\left(\frac{u_{bj}^2}{u_{\xi jmax}^2} + k_{b\xi j}^2 - 1\right) + \frac{c_{2\xi j}u_{bj}k_{b\xi j}}{u_{\xi jmax}^2}\left(u_{bj} - u_{\xi j}\right) \quad (39)$$

with $c_{1\xi j}$, $c_{2\xi j}$ being positive constants, $j = 1,\ 2$. Then, the UDE-based altitude controller $F = u_{\xi 3}$ is designed as

$$F = B_{\xi 3}^{-1}\hat{g}_3 - B_{\xi 3}^{-1}\{k_{b\xi 3}k_{\xi 3}\varepsilon_{\xi 3} + \lambda_{\xi 3}\dot{e}_{\xi 3} + \ddot{\xi}_{r3} + \mathcal{L}^{-1}\left[\frac{G_{\xi 3}^{f}(s)}{1-G_{\xi 3}^{f}(s)}\right] * \left[\dot{\varepsilon}_{\xi 3} + k_{b\xi 3}k_{\xi 3}\varepsilon_{\xi j3}\right]\} \quad (40)$$

C. Boundedness Analysis

Through the bounded UDE-based position controller (36)-(39), the references for roll and pitch angles will be bounded. The detailed analysis is given as follows. Consider the following Lyapunov function candidate as

$$V_j = \frac{u_{bj}^2}{u_{\xi jmax}^2} + k_{b\xi j}^2 \ \ (j = 1,\ 2) \quad (41)$$

Taking the time derivative of V_j and then combining (38) and (39) yield

$$\dot{V}_j = -2c_{1\xi j}\left(\frac{u_{bj}^2}{u_{\xi jmax}^2} + k_{b\xi j}^2\right)\left(\frac{u_{bj}^2}{u_{\xi jmax}^2} + k_{b\xi j}^2 - 1\right) \quad (42)$$

From (42), it can be observed that the sign of $\dot{V}_j$ is related to an ellipse at the point $(0,\ 0)$ defined by

$$C = \left\{u_{bj},\ k_{b\xi j} \in R : \frac{u_{bj}^2}{u_{\xi jmax}^2} + k_{b\xi j}^2 = 1\right\} \quad (43)$$

The derivative of the Lyapunov function, $\dot{V}_j$, obeys the conditions as follows: $\dot{V}_j < 0$ outside the ellipse C and $\dot{V}_j > 0$ inside of the ellipse except from the origin where it is zero.

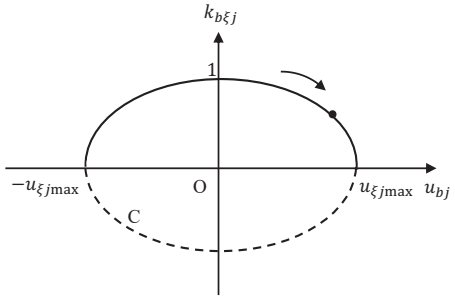

Figure 3. Boundedness of u_{bj}

This means once u_{bj} goes outside of the ellipse, it will be back on the ellipse and stay on the ellipse, as shown in Fig. 3. This property guarantees that the virtual output u_{bj}, $j = 1,\ 2$, is bounded within the constrained range $(-u_{\xi jmax},\ u_{\xi jmax})$. According to the position control output (36)-(37), the values $u_{\xi 1max}$ and $u_{\xi 2max}$ can be selected as $u_{\xi 1max} = \theta_{max}K_x$ and $u_{\xi 2max} = \phi_{max}K_y$, such that $\phi_r \in (-\phi_{max},\ \phi_{max})$, $\theta_r \in (-\theta_{max},\ \theta_{max})$ are satisfied.

Define the UDE estimation error as $\tilde{D}_{\eta i} = D_{\eta i} - \hat{D}_{\eta i}$. Replacing $D_{\eta i}$ with $\hat{D}_{\eta i}$ in (24) along (22) leads to

$$\dot{\varepsilon}_{\eta i} = -k_{\eta i}\varepsilon_{\eta i} - \tilde{D}_{\eta i} \quad (i = 1,\ 2) \quad (44)$$

Substituting (21) into (44) results in

$$\ddot{e}_{\eta i} = -k_{\eta i}\lambda_{\eta i}e_{\eta i} - \left(k_{\eta i} + \lambda_{\eta i}\right)\dot{e}_{\eta i} - \tilde{D}_{\eta i} \quad (45)$$

Combining (27) and (28), there is

$$\tilde{D}_{\eta i} = D_{\eta i} * L^{-1}\left[1 - G_{\eta i}^{f}(s)\right] \quad (46)$$

Substituting (46) into (45) and then taking the Laplace transformation

$$s^2E_{\eta i}(s) = -k_{\eta i}\lambda_{\eta i}E_{\eta i}(s) - \left(k_{\eta i} + \lambda_{\eta i}\right)sE_{\eta i}(s) - \mathbf{D}_{\eta i}(s)\left[1 - G_{\eta i}^{f}(s)\right] \quad (47)$$

where $E_{\eta i}(s)$ and $\mathbf{D}_{\eta i}(s)$ are the Laplace transform of $e_{\eta i}$ and $D_{\eta i}$, respectively. If the filters $G_{\eta i}^{f}(s)$ are designed as strictly proper stable filters with $G_{\eta i}^{f}(0) = 1$, by applying the final value theorem to (47), there is

$$\begin{aligned}\lim_{t\to\infty} e_{\eta i} &= \lim_{s\to 0} s\cdot E_{\eta i}(s) \\ &= \lim_{s\to 0} -s\cdot\frac{\mathbf{D}_{\eta i}(s)\left[1 - G_{\eta i}^{f}(s)\right]}{\left[s^2 + \left(k_{\eta i} + \lambda_{\eta i}\right)s + k_{\eta i}\lambda_{\eta i}\right]} \\ &= 0\end{aligned} \quad (48)$$

Hence, the mean values of the tracking errors for both roll angle ϕ and pitch angle θ converge to zero. It can be concluded that, by using the bounded UDE-based position controller (36)-(39) and the UDE-based attitude controller (30), both ϕ and θ are constrained, i.e., $\phi \in (-\phi_{max},\ \phi_{max})$, $\theta \in (-\theta_{max},\ \theta_{max})$.

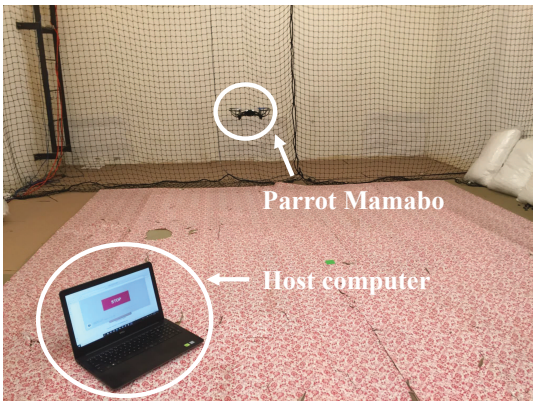

Figure 4. Experimental setup

Table I
CONTROL PARAMETERS

i/j	$\lambda_{\eta i}$	$\lambda_{\xi j}$	$T_{\eta i}$	$T_{\xi j}$	$k_{\eta i}$	$k_{\xi j}$	$c_{1\xi j}$	$c_{2\xi j}$
1	0.01	0.01	0.01	0.01	0.22	0.02	100	50
2	0.01	0.01	0.01	0.01	0.22	0.02	100	50
3	0.01	0.01	0.02	0.02	0.22	0.02	-	-

IV. EXPERIMENTAL RESULTS

In this section, the proposed bounded UDE-based control is implemented on a platform, Parrot Mambo [21]. The platform is equipped with one down facing camera and one ultrasound sensor for position sensing. The dimension is 18cm×18cm and the weight is 73g. The host computer is in charge of sending the takeoff command to the Parrot Mambo. The experimental setup is shown in Fig. 4. The comparison with the traditional UDE-based control [18] is provided to illustrate the effectiveness of the proposed bounded UDE-based control.

A. Filter Design and Parameter Selection

According to the guidance of the filter design mentioned in [22], the filters in the UDE-based controllers are chosen as

$$G^f_{\eta i}(s) = \frac{1}{T_{\eta i}s + 1} \quad (i = 1,\ 2,\ 3) \tag{49}$$

$$G^f_{\xi j}(s) = \frac{1}{T_{\xi j}s + 1} \quad (j = 1,\ 2,\ 3) \tag{50}$$

where $T_{\eta i}$ and $T_{\xi j}$ are positive constants. The control parameters of the proposed bounded UDE-based control strategy are listed in Table I. For a fair comparison, the traditional UDE controller use the same parameter selection. The constants K_x and K_y are set as $K_x = K_y = 1$ and $I_x = 0.00005829\,\mathrm{kg}\cdot\mathrm{m}^2$, $I_y = 0.00007169\,\mathrm{kg}\cdot\mathrm{m}^2$, $I_z = 0.00001\,\mathrm{kg}\cdot\mathrm{m}^2$, $g = 10\,m/s^2$, $m = 0.073\,\mathrm{kg}$.

Moreover, the constraints for both roll and pitch angles are chosen as $\phi_{max} = \theta_{max} = 12°$, based on the experimental testings, so that a SLAM system will not suffer the pose lost within these constraints.

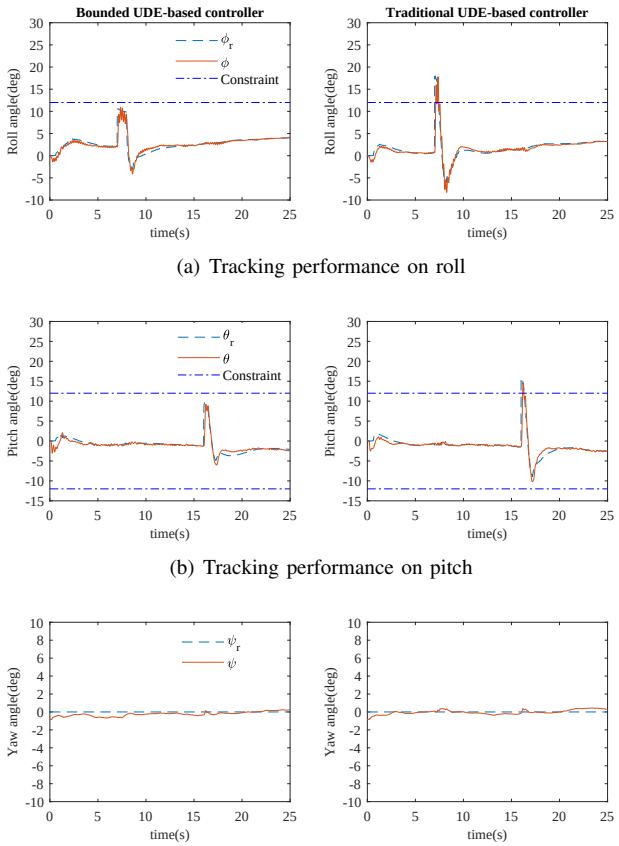

(a) Tracking performance on roll

(b) Tracking performance on pitch

(c) Tracking performance on yaw

Figure 5. Attitude tracking performance

B. Control Performance

The waypoint tracking is commonly used in most of SLAM systems. In this section, a three-waypoint trajectory is chosen. The starting point is set up as $[x,\ y,\ z] = [0,\ 0,\ 0.8]$, and the first, second and third waypoints as $[-0.1,\ -0.1,\ 0.8]$, $[-0.1,\ 0.9,\ 0.8]$ and $[-1.1,\ 0.9,\ 0.8]$, which are indicated in Fig. 6(d).

The first waypoint is given at $t = 1s$. The quadrotor will take off first and hover to wait for the next waypoint command. The second waypoint is given at $t = 7s$. As shown in the left column of Fig. 5(a), the controller output of the bounded UDE-based controller, ϕ_r, is always within the given constraint. However, the output of the traditional UDE controller shown in the right column of Fig. 5(a) violates the constraint. The third waypoint is given at $t = 16s$. As shown in the left column of Fig. 5(b), the output of the bounded UDE based-controller, θ_r, never breaks the constraint, however, the traditional UDE controller does as shown in right column of Fig. 5(b). Fig. 5(c) shows that both controllers can successfully track the reference signal ψ_r. From the above results, it can be concluded that, with the implementation of the proposed bounded UDE-based controller, the desired controller outputs will always remain within the given bounds.

The position tracking performance comparison between the

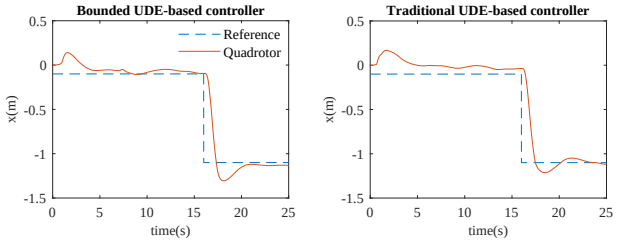

(a) Tracking performance on x

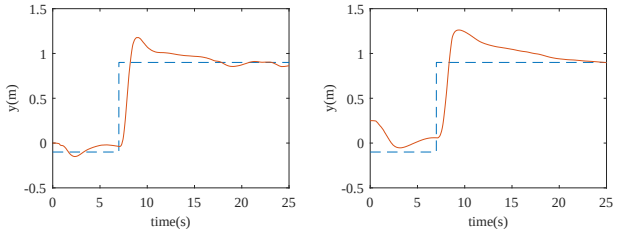

(b) Tracking performance on y

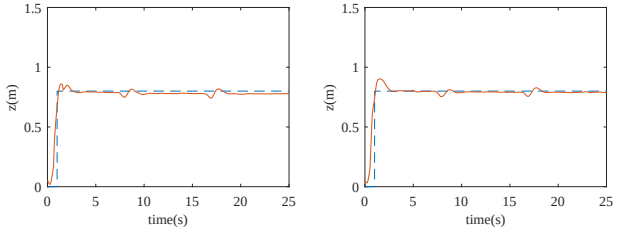

(c) Tracking performance on z

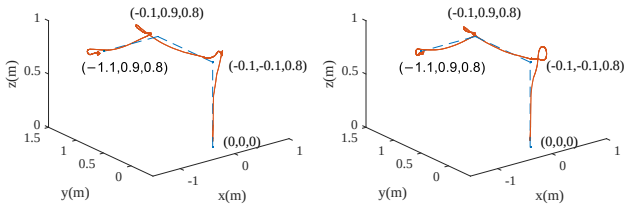

(d) Tracking performance in 3D space

Figure 6. Position tracking performance

proposed bounded UDE-based controller and the traditional UDE-based controller is provided in Fig. 6. As shown in Fig. 6(a), (b) and (c), the steady state position tracking performance of both controllers on x, y and z are similar and can converge to the neighborhood of zero eventually. However, the proposed bounded UDE-based controller has faster response than the traditional UDE-based controller. Fig. 6(d) shows the overall tracking performance in 3D space.

V. Conclusion

In this paper, a bounded UDE-based control strategy has been developed to provide a suitable platform for a quadrotor carried SLAM system. With the implementation of the proposed control strategy, both roll and pitch angles of the quadrotor have been regulated within appropriate ranges, which ensures the elimination of the sudden motion. Finally, the experimental results have demonstrated the effectiveness of the proposed controller for handling the constraint regulation and the waypoint tracking assignment.

References

[1] A. J. Davison, I. D. Reid, N. D. Molton, and O. Stasse, "MonoSLAM: Real-time single camera SLAM," *IEEE Trans. Pattern Anal. Mach. Intell.*, no. 6, pp. 1052–1067, 2007.

[2] M. J. Milford and G. F. Wyeth, "Mapping a suburb with a single camera using a biologically inspired SLAM system," *IEEE Trans. Robot.*, vol. 24, no. 5, pp. 1038–1053, 2008.

[3] R. Mur-Artal, J. M. M. Montiel, and J. D. Tardos, "ORB-SLAM: a versatile and accurate monocular SLAM system," *IEEE Trans. Robot.*, vol. 31, no. 5, pp. 1147–1163, 2015.

[4] S. Weiss, D. Scaramuzza, and R. Siegwart, "Monocular-SLAM–based navigation for autonomous micro helicopters in GPS-denied environments," *IEEE Trans. Robot.*, vol. 28, no. 6, pp. 854–874, 2011.

[5] B. Williams, G. Klein, and I. Reid, "Automatic relocalization and loop closing for real-time monocular SLAM," *IEEE Trans. Pattern Anal. Mach. Intell.*, vol. 33, no. 9, pp. 1699–1712, 2011.

[6] G. Klein and D. Murray, "Improving the agility of keyframe-based SLAM," in *European Conference on Computer Vision*. Springer, 2008, pp. 802–815.

[7] B. Williams, P. Smith, and I. Reid, "Automatic relocalisation for a single-camera simultaneous localisation and mapping system," in *IEEE Conf. Robotics and Automation*. IEEE, 2007, pp. 2784–2790.

[8] G. Reitmayr and T. Drummond, "Going out: robust model-based tracking for outdoor augmented reality," in *IEEE and ACM International Symposium on Mixed and Augmented Reality*. IEEE Computer Society, 2006, pp. 109–118.

[9] B. Williams, G. Klein, and I. Reid, "Real-time SLAM relocalisation," in *IEEE International Conference on Computer Vision*. IEEE, 2007, pp. 1–8.

[10] S. Zhu, D. Wang, and C. B. Low, "Ground target tracking using UAV with input constraints," *Journal of Intelligent & Robotic Systems*, vol. 69, no. 1-4, pp. 417–429, 2013.

[11] W. Ren and R. W. Beard, "Trajectory tracking for unmanned air vehicles with velocity and heading rate constraints," *IEEE Trans. Control Syst. Technol.*, vol. 12, no. 5, pp. 706–716, 2004.

[12] N. Cao and A. F. Lynch, "Inner–outer loop control for quadrotor UAVs with input and state constraints," *IEEE Trans. Control Syst. Technol.*, vol. 24, no. 5, pp. 1797–1804, 2016.

[13] S. Zhu and D. Wang, "Adversarial ground target tracking using UAVs with input constraints," *Journal of Intelligent & Robotic Systems*, vol. 65, no. 1-4, pp. 521–532, 2012.

[14] T.-T. Tran, S. Sam, W. He, P. Luu-Trung-Duong, and N.-V. Truong, "Trajectory tracking control of a quadrotor aerial vehicle in the presence of input constraints," *International Journal of Control, Automation and Systems*, vol. 16, no. 6, pp. 2966–2976, 2018.

[15] D. Liu, X. Yang, D. Wang, and Q. Wei, "Reinforcement-learning-based robust controller design for continuous-time uncertain nonlinear systems subject to input constraints," *IEEE Trans. Cybern.*, vol. 45, no. 7, pp. 1372–1385, 2015.

[16] Q.-C. Zhong and D. Rees, "Control of uncertain LTI systems based on an uncertainty and disturbance estimator," *ASME Trans. J. Dyn. Sys. Meas. Control*, vol. 126, no. 4, pp. 905–910, Dec. 2004.

[17] Q. Lu, B. Ren, and S. Parameswaran, "Shipboard Landing Control Enabled by an Uncertainty and Disturbance Estimator," *Journal of Guidance, Control, and Dynamics*, vol. 41, no. 7, pp. 1502–1520, 2018.

[18] Q. Lu, B. Ren, S. Parameswaran, and Q.-C. Zhong, "Uncertainty and disturbance estimator-based robust trajectory tracking control for a quadrotor in a global positioning system-denied environment," *Journal of Dyn. Sys. Meas. Con.Trans. ASME*, vol. 140, no. 3, p. 031001, 2018.

[19] R. Sanz, P. Garcia, Q.-C. Zhong, and P. Albertos, "Predictor-based control of a class of time-delay systems and its application to quadrotors," *IEEE Trans. Ind. Electron.*, vol. 64, no. 1, pp. 459–469, 2017.

[20] Y. Wang, B. Ren, and Q.-C. Zhong, "Bounded UDE-based controller for systems with input constraints," in *Proc. 57th IEEE Conf. Decision and Control*, Dec. 2018, pp. 2976–2981.

[21] PARROT MAMBO FPV. [Online]. Available: www.parrot.com/us/drones/parrot-mambo-fpv

[22] B. Ren, Q.-C. Zhong, and J. Dai, "Asymptotic reference tracking and disturbance rejection of UDE-based robust control," *IEEE Trans. Ind. Electron.*, vol. 64, no. 4, pp. 3166–3176, Apr. 2017.